Atomic Data Needs for X-ray Astronomy. 22 June 2000
http://heasarc.gsfc.nasa.gov/docs/heasarc/atomic/
M. A. Bautista, T. R. Kallman, and A. K. Pradhan, eds.

K-Shell Photoionization of Fe

B M McLaughlin[1], D Donnelly[1], K L Bell[1], M P Scott[1] and F P Keenan[2]
[1]*Department of Applied Mathematics and Theoretical Physics*
[2]*Department of Pure and Applied Physics*
The Queen's University of Belfast, Belfast BT7 1NN, N. Ireland

Abstract. The status of K-shell photoionization of neutral iron has been reviewed. A comparison with the available experimental data and existing theoretical work is made for this important element. Several anomalies and features are illustrated and future directions of theoretical work are indicated.

1. Introduction

The *Ginga* satellite, launched in 1987, provided the first indication that the X-ray spectra of active galactic nuclei (AGN) were not featureless continua, but also contained structure associated with various atomic processes. Iron Fe-K emission lines (H-like, FeXXVI and He-like, FeXXV) with wavelengths of 1.936 Åand 1.940 Å were observed (Mushotzky et al. 1993). These lines are characteristic of X-ray illuminated cold material, and act as an indication of the amount of cool material illuminated by the AGN. More recently launched X-ray satellites, *Chandra*, July 23, 1999 and *XMM*, December 10, 1999 for the first time provide the ability to do X-ray spectroscopy in very high resolution. Elements of prime interest are C, N, O, Ne, Mg, Si, S, Ca, Ar, Fe and Ar, primarily at the K and L-edge energies for a number of ionization stages and a wide range of energies (0.1 - 12 keV). With the advent of such high resolution spectra there is an urgent need for high quality atomic data for photon and electron collisional excitation on the atomic species of interest together with their respective transitions probabilities.

Fe-K lines are observed in solar flares and are produced within the solar photosphere by the hot plasma in the corona (Bai 1979; Parmar et al. 1984; Phillips et al. 1994) and in active galactic nuclei (AGN). The appearance of these lines is due to the $2p \rightarrow 1s$ transition, which spontaneously occurs as a result of the instability of the $1s$ hole states generated from the K-shell photoionization of neutral iron. This instability is due to the large binding energy of the Fe $1s$ shell ($\sim$ 7 keV), the magnitude of which presents a major obstacle to determining accurate experimental or theoretical data for the K-shell photoionization of neutral iron.

The importance of understanding what occurs when high energy photons collide with neutral iron have many applications. It is known that in the interstellar medium, iron (Fe), silicon (Si) and magnesium (Mg) appear mainly at the same order of abundance in silicate grains. All Fe ions can emit K-shell photons in the region around the Fe-K emission region, the average energy of which moves from 6.4 keV to 6.7 keV as the ionization stage increases. Only in high resolution with statistics folded in will it confirm if neutral Fe K-shell lines are present in the spectra. Furthermore, X-ray Fluorescence in dark clouds (that is secondary emitted photons as a result of inner shell rearrangements by the incident photon) is important to understand so as to build accurate theoretical models. Figure 1 illustrates the presence of the Fe (K_α) line and its bremsstrahlung continua, in the spatial resolution of the ground based detector calibration for the Chandra satellite. The results are for an non-flight camera, the High Speed Imager (HSI) which shows a quasi-Gaussian peak with the approximate width for the telescope point spread function. The Fe (K_α) line is clearly visible as is the corresponding weaker bremsstrahlung continua (Edgar 1999, private communication). The setup includes an electron-ion point source (EIPS) with an iron anode which produces neutral Fe K and L lines and a bremsstrahlung continuum, and a filter of Mn with a thickness of about 2 mean free paths at 6.4 keV which has its K-edge between Fe K_α and K_β. The Mn filter also cuts out a large part of the continuum making a source spectrum strongly dominated by the one line, in this case the Fe K_α at 6.4 keV. Finally another interesting quantity to

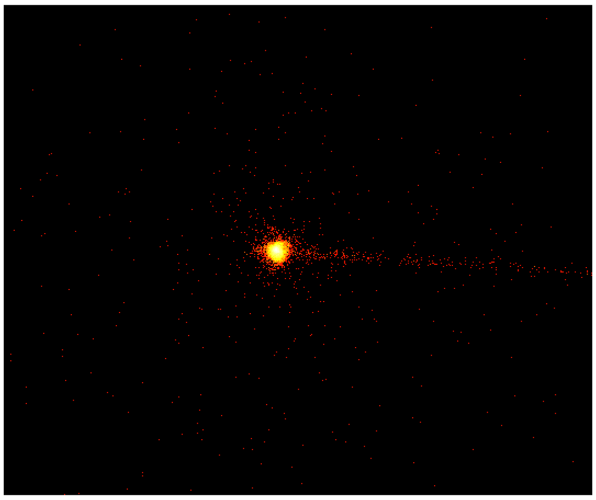

Figure 1. Ground base calibration of the detector for the Chandra satellite. The neutral iron (Fe) K_α line is clearly visible (bright spot) as is the corresponding weaker continuum bremsstrahlung tail to it's right; courtesy of the SAO/MIT/Marshall Space Flight Center calibration group (Edgar 1999, private communication).

know is what is the total Fe abundance. Astrophysically, neutral iron is rare. However in the ultra-violet (UV) region singly ionized iron (Fe^{+}) has been observed in the Gas Phase but in the solid state phase the amount of Fe present is very much open to interpretation and speculation (Raymond and Smith 1999, private communication).

2. Overview of previous work

In order to assess the level of sophistication required in a theoretical model of neutral iron one first has to assess the status of theoretical work on this complex element. The first calculations on this complex system were made using the relativistic central field Dirac-Slater approximation (Verner et al. 1993; Verner and Yakovlev 1995). Verner and co-workers calculated the cross-section for the 1*s*-photoionization of neutral iron (Fe) as part of a more general study of photoionization from each individual sub-shell of ions of elements between helium and zinc. The results were found to have an approximate linear dependence on the photon energy. For valence shell photoionization the first attempt to treat this complex at the ab initio level was carried out by Bautista and Pradhan (Bautista and Pradhan 1995). These photoionization calculations catered only for the outer (valence) shell electrons of Fe but however showed a discrepancy of several orders of magnitude compared with the results relativistic central field approximation (Verner et al. 1993).

Recently ab initio work on inner shell photoionization of this complex system was carried out by Black and co-workers (Black et al. 1998) within the context of the R-matrix approach (Burk and Berrington 1993). In that work nine $1s^{-1}$ target hole states of Fe^+ were used obtained from the base configuration $1s^{-1}3d^64s^2$ for the photoionization calculations. Each of the nine-states were represented by a single configuration and electron correlation effects from configuration interaction mixing were neglected. The ground state of neutral iron was represented by a single configuration and no autoionizing states were considered. The results showed (as illustrated in Figure 2) that the relativistic central field approximation were essentially 'duplicated' at an energy of 1.25 keV above the lowest $1s^{-1}3d^64s^2$ hole state of Fe^+ included. The ab initio R-matrix method was used in order to test the viability of including $1s$ hole states of Fe^+ only in the calculation of K-shell photoionization cross sections. Despite the requirement of a large (sixty-four) number of continuum orbitals, the results were highly satisfactory with excellent agreement with the work of Verner and co-workers (Verner et al. 1993) occurring at higher photon energies as is seen from Figure 2. The results of Black and co-workers (Black et al. 1998) demonstrated an unusually rapid growth near the threshold which appeared to be inconsistent with the cross sections found experimentally for structurally similar neutral nickel (Parthasaradhi et al. 1998).

3. Ab initio Work

Following the work of Black and co-workers further investigations were carried out (Donnelly et al. 1999, 2000). Many sophisticated theoretical approaches have difficulties in dealing with such deep inner shell electron excitation. In particular, the R-matrix method encounters problems in so far as the number of continuum orbitals required to span the energy range between the the neutral Fe ground state and the $1s$ hole states of Fe^+ is quite considerable. A further difficulty in applying any close-coupling approximation to this problem is in the determination of the actual target $1s^{-1}$ hole states of Fe^+ to be included in the wavefunction expansion. A more realistic description of the process is attempted by including the 'ground' $1s^{-1}$ hole Fe^+ state together with excited hole states, each target state being represented by a configuration interaction type wave function, in an attempt to either confirm or refute the rapid growth feature in the calculations of Black and co-workers (Black et al. 1998). Sixteen $1s^{-1}$-hole Fe^+ target states are utilized, with each one represented by an extensive configuration interaction. Electron correlation effects significantly alter the magnitude of the background cross section in comparison with earlier work and extensive resonance structure is resolved near the lowest threshold of the $1s^{-1}$-hole Fe^+ state as is illustrated in Figure 3. The ground state of the neutral Fe is represented in this manner so that one keeps the Fe and Fe^+ systems 'balanced' by treating the neutral Fe ground state as a bound state of the $\{Fe^+ + e^-\}$ system.

3.1. Target States of Fe^+

Our calculations adopt a similar approach to the one used by Black and co-workers (Black et al. 1998) where the Fe^+ ground state is omitted and only a selected number of $1s^{-1}$ hole states of Fe^+ as target states are included. This choice of target states requires consideration of the following inner-shell processes:

$$h\nu + \mathrm{Fe}\left\{1s^22s^22p^63s^23p^63d^64s^2\ {}^5D\right\}$$

$$\downarrow$$

$$\mathrm{Fe}^+\left\{\begin{array}{c} 1s2s^22p^63s^23p^63d^8\ {}^{2S+1}L \\ 1s2s^22p^63s^23p^63d^74s\ {}^{2S+1}L \\ 1s2s^22p^63s^23p^63d^64s^2\ {}^{2S+1}L \end{array}\right\} + e^- \tag{1}$$

In total twenty-three target states result from the photon ejection processes outlined in 1. From the work of Black and co-workers (Black et al. 1998) which included only the hole states $1s^{-1}3d^64s^2$, it was demonstrated that $1s^{-1}3d^6(^5D)4s^2\ {}^6D$ and ${}^4D$ states only contribute significantly to the cross section. Hence of the nine-states of this type, only these two states are included leaving a total of sixteen target hole states. The configurations used to represent these target state wave functions are generated from the set of one-electron orbitals $\{1s, 2s, 2p, 3s, 3p, 3d, 4s, \overline{4p}, \overline{4d}, \overline{5s}, \overline{5d}\}$, whose radial part is represented by a linear combination of Slater-type orbitals. The $1s$, $2s$, $2p$, $3s$ and $3p$ orbitals are the Hartree-Fock ground state orbitals of Fe^+ (Clementi and Roetti 1974), while the remaining orbitals were generated by energy optimizing the radial functions using the atomic structure code CIV3 (Hibbert 1975).

The $3d$ and $4s$ orbitals were energy optimized on the Fe^+ $1s^{-1}3d^74s$ ^6F state. The optimal $3d$ orbital obtained in this manner is highly satisfactory for all $1s$ hole states with a valence electron arrangement of $1s^{-1}3d^74s$. However it differs significantly from the optimal form of the $1s$ hole states, with the valence electron arrangement of $1s^{-1}3d^8$. Consequently, we optimize a $\overline{4d}$ orbital on $1s^{-1}3d^8$ ^4F using two configurations: $1s^{-1}[3d^8 + 3d^7\overline{4d}]$ ^4F. Furthermore it is also observed that the $3d$ orbital being used differs from the optimal $3d$ found in states which are of the form $1s^{-1}3d^64s^2$, while the $4s$ also differs from the optimal $4s$ of these types of states. We thus determine further corrector orbitals for each of these cases, by simultaneously optimizing a $\overline{5s}$ and $\overline{5d}$ corrector orbital on the $1s^{-1}3d^64s^2$ ^6D state using the following set of configurations: $1s^{-1}[3d^64s^2 + 3d^64s\overline{5s} + 3d^64s\overline{4d} + 3d^64s\overline{5d} + 3d^54s^2\overline{4d} + 3d^54s^2\overline{5d}]$ ^6D. Finally, further valence shell correlation is introduced by using a $\overline{4p}$ pseudo orbital which is optimized on the $1s^{-1}3d^64s^2$ ^6D state also, but this time we only use the following two configurations: $1s^{-1}[3d^64s^2 + 3d^6\overline{4p}^2]$ ^6D. The resulting parameters for this and the other optimized orbitals are given in Table 1.

Table 1. Radial function parameters for Fe^+ orbitals.

nl	c_j	I_j	ζ_j	$<r>$	nl	c_j	I_j	ζ_j	$<r>$
$3d$	0.03953	3	11.71760	0.96202	$\overline{4p}$	0.13463	2	11.63605	2.68050
	0.31529	3	6.21570			-0.33988	3	4.93808	
	0.32377	3	4.06451			1.00840	4	1.66329	
	0.39096	3	2.54111						
	0.08377	3	1.60897		$\overline{4d}$	0.45825	3	5.44096	2.50343
						-0.94999	4	1.62731	
$4s$	0.00469	1	39.07900	2.81236					
	-0.04064	1	25.59940		$\overline{5s}$	0.28429	1	10.52423	2.68076
	-0.01141	2	21.70570			-0.65984	2	10.43637	
	0.11936	2	10.88620			0.77988	3	6.09671	
	0.06587	3	9.40162			-1.08361	4	2.64182	
	-0.06104	3	7.05231			0.89168	5	1.45405	
	-0.30777	3	4.71260						
	0.03839	4	3.83931		$\overline{5d}$	0.54078	3	6.73270	2.57939
	0.67820	4	1.86530			-7.66811	4	1.39691	
	0.40217	4	1.19327			7.99473	5	1.61600	
	-0.02782	4	0.83151						

With this set of atomic orbitals, the configuration state functions (CSF's) are generated by adding one electron from the orbital basis set, with the exception of the $1s$ orbital, to the following basis distributions; $1s^{-1}3d^7$, $1s^{-1}3d^64s$, $1s^{-1}3d^54s^2$ and the $1s^{-1}3d^6\overline{4p}^2$ hole states configurations for electron correlation purposes. Only the even configurations are considered from this procedure, since all of our target states are of that parity which results in a total of 763 configurations. The eigenenergies of the target states were determined using the atomic structure computer code CIV3 (Hibbert 1975) and are presented in Table 2 relative to the lowest Fe^+ hole state. To our knowledge, no experimental data exist for comparison purposes of all these states and in particular the excited hole states of Fe^+. We note it is essential to include pseudo-orbitals in order to achieve an accurate description of the target states and that the use of spectroscopic orbitals only cannot fully account for the various correlations occurring in the states resulting from the different core rearrangements.

3.2. Photoionization Calculations

The electron configurations for the neutral Fe in the present calculation are generated by the addition of one electron from the orbital basis set to the target state configurations included in the calculations. Here

Table 2. Fe^{+} term energies relative to the lowest $1s^{-1}3d^{8}$ hole state

Target State	Energy (a.u.)	Energy (Ryd)	Energy (eV)
$1s^{-1}3d^{8}\ {}^{4}F$	0.000000	0.000000	0.0000000
$1s^{-1}(3d^{7}\ {}^{4}F)({}^{5}F)4s\ {}^{6}F$	0.058532	0.117064	1.5927374
$1s^{-1}(3d^{7}\ {}^{4}F)({}^{3}F)4s\ {}^{4}F$	0.066235	0.132470	1.8023468
$1s^{-1}3d^{8}\ {}^{4}P$	0.070907	0.141814	1.9294785
$1s^{-1}(3d^{7}\ {}^{5}F)4s\ {}^{4}F$	0.088616	0.177232	2.4113651
$1s^{-1}(3d^{7}\ {}^{4}P)({}^{5}P)4s\ {}^{6}P$	0.140332	0.280664	3.8186296
$1s^{-1}(3d^{7}\ {}^{4}P)({}^{3}P)4s\ {}^{4}P$	0.148154	0.296308	4.0314772
$1s^{-1}(3d^{7}\ {}^{2}G)({}^{3}G)4s\ {}^{4}G$	0.157481	0.314962	4.2852779
$1s^{-1}(3d^{7}\ {}^{4}P)({}^{5}P)4s\ {}^{4}P$	0.171142	0.342284	4.6570127
$1s^{-1}(3d^{7}\ {}^{2}H)({}^{3}H)4s\ {}^{4}H$	0.184958	0.369916	5.0329654
$1s^{-1}(3d^{7}\ {}^{2}P)({}^{3}P)4s\ {}^{4}P$	0.185816	0.371632	5.0563128
$1s^{-1}(3d^{7}\ a^{2}D)({}^{3}D)4s\ {}^{4}D$	0.195742	0.391484	5.3264131
$1s^{-1}(3d^{6}\ {}^{5}D)({}^{6}D)4s^{2}\ {}^{6}D$	0.266753	0.533506	7.2587215
$1s^{-1}(3d^{7}\ {}^{2}F)({}^{3}F)4s\ {}^{4}F$	0.268866	0.537732	7.3162192
$1s^{-1}(3d^{6}\ {}^{5}D)({}^{4}D)4s^{2}\ {}^{4}D$	0.271122	0.542244	7.3776081
$1s^{-1}(3d^{7}\ b^{2}D)({}^{3}D)4s\ {}^{4}D$	0.384466	0.768932	10.461857

we allow the addition of a $1s$ orbital, which results in the generation of the $1s^{2}2s^{2}2p^{6}3s^{2}3p^{6}3d^{7}4s\ {}^{5}D$ ground state configuration of neutral Fe and its associated electron correlation configurations, as well as the $1s^{-1}$ hole states of both even and odd parity generated by the addition of the other orbitals in the basis set. These odd parity configurations are bound state configurations which are used in the representation of the autoionizing states have $LS\pi$ symmetry values of ${}^{5}P^{o}$, ${}^{5}D^{o}$ and ${}^{5}F^{o}$. This approach results in a 'balanced' set of configurations for the neutral and single ionized Fe systems. With a R-matrix boundary radius of 12.3 Bohr it required a minimum of sixty-continuum orbitals for each value of the free electron orbital angular momentum ℓ ($\ell \leq 8$), to span the outgoing electron energy range of $\sim$ 1.65 keV relative to the lowest lying $1s^{-1}3d^{8}$ hole state. The K-edge energy for neutral Fe was calculated to be 7.084 keV in suitable agreement with the 7.083 keV theoretical estimate of Verner and

Table 3. K-edge energies for neutral Fe.

Method	Energy (keV)	Energy (Ryd)
9CC [1]	7.1112	522.69
16CC [2]	7.0840	520.69
DS [3]	7.0830	520.61
EXPT [4]	7.1240	523.63
EXPT [5]	7.1160	523.04
EXPT [6]	7.1120	522.75
EXPT [7]	7.1150	522.97
EXPT [8]	7.1140	522.89

[1] Theory: 9-state R-matrix LS coupling
[2] Theory: 16-state R-matrix LS coupling
[3] Theory: DS Central Field Approximation (Verner et al. 1993)
[4] Experiment (Gas) (Servier 1979)
[5] Experiment (Solid) (Servier 1979)
[6] Experiment (Solid) (Servier 1979)
[7] Experiment (Oxide) (Servier 1979)
[8] Henke's Tables (Henke et al. 1993)

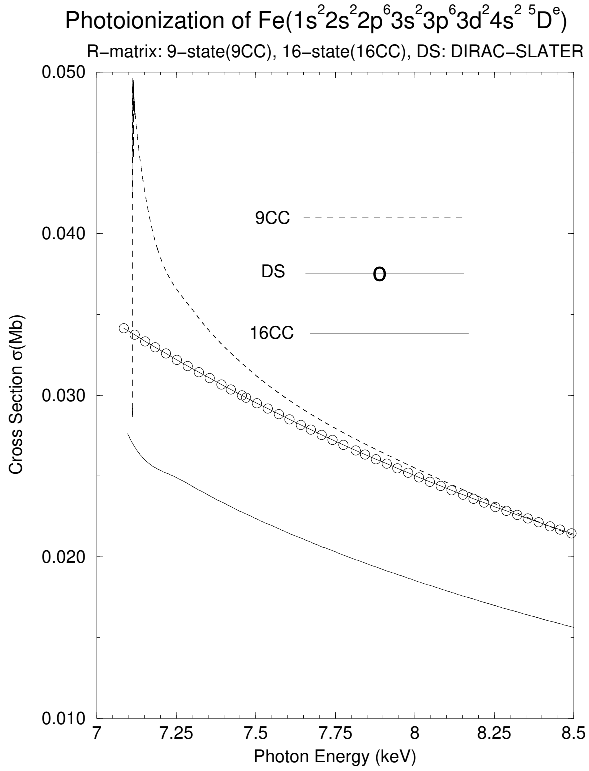

Figure 2. Total cross sections for the 1s photoionization of the ground state of neutral iron. Solid line is the 16-state results, for energies (keV) above the hole states, dashed line is that from the 9-state work (Black et al. 1998) and the open circles are those from the relativistic central field approximation (Verner et al. 1993).

co-workers (Verner et al. 1993) and in respectable accord with the available experimental measurements of Servier and co-workers (Servier 1979) and that given in Henke's tables (Henke et al. 1993) and are presented in Table 3.

4. Results

The total $1s^{-1}$ photoionization cross section is calculated by summing the individual contributions from each of the inner-shell processes in equation (1) and including only the two dominant contribution from the $1s^{-1}3d^6 4s^s$ hole states. For the photon energy region from threshold to the highest hole-state included in the calculation an energy resolution of 1.36 meV (10^{-4} Rydbergs) is used to fully resolve the expected resonance structure. Above this region a larger step length of 0.136 eV (10^{-2} Rydbergs) is employed. The sixteen-state results using the length formulation are given in Figures 2 and 3 and are compared with the nine-state results of Black and co-workers (Black et al. 1998) and those from the relativistic central field Dirac-Slater approximation of Verner and co-workers (Verner et al. 1993).

Some striking differences are evident among the three sets of results. The sixteen-state results are unique in that they demonstrate very extensive resonance structure in photon energy region the 7084.351 eV ($\sim$ 520.69 Rydbergs) to 7094.827 eV ($\sim$ 521.46 Rydbergs) as is illustrated in Figure 4. All three symmetries ($^5F^o$, $^5D^o$ and $^5P^o$) that contribute to the total inner-shell photoionization cross section exhibit strong resonance structure with autoionizing resonance series approaching the $1s^{-1}$ hole state thresholds. These autoionization resonances are of the form $1s^{-1}3d^7 4snp, nf, \ldots$, $1s^{-1}3d^6 4s^2 np, nf, \ldots$ and $1s^{-1}3d^8 np, nf \ldots$ caused by the electron being able to attach itself to the $1s^{-1}$ hole states. These resonances represent the autoionizing states as generated by the method described previously. Figure 2 illustrates the region above all the hole states included in the 16-state work whereas Figure 3 displays the photoabsorption cross section for the entire energy region studied, where the energy unit is now given in Rydbergs, From Figures 2, 3 and 4 some striking differences are evident among the three sets of results. Firstly, the sixteen-state results demonstrate extensive resonance structure in the photon energy region 7.084 keV to 7.095 keV as seen in Figure 4. We note that, while of a smaller magnitude, the large jump in the cross section which occurs in the nine-state work at the $1s^{-1}3d^6 4s^2\ ^6D$ and ^4D thresholds (photon energy 7091.562 eV and 7091.698 eV respectively) is also present in the sixteen-state calculation (see Figure 4). It was found that with the exception of some resonance structure, the remaining target states of the form $1s^{-1}3d^8$ and $1s^{-1}3d^7 4s$ had a negligible contribution to the total background cross section. The $1s^{-1}3d^6 4s^2$ target states by far give the major contribution to the background cross section as illustrated in Figure 5 compared to the $1s^{-1}3d^8$ states (cf Figure 6) or the $1s^{-1}3d^7 4s$ states (cf Figure 7). Of consequence to astrophysical modelers, is the fact that throughout the energy range considered the present background cross section lies at best $\sim$ 20%, and at worst $\sim$ 30%, lower than the work of Verner and co-workers (Verner et al. 1993). However, the energy difference between the two sets of data is slowly decreasing, so that at much higher photon energies the two calculations will converge. At higher energies the results of Black and co-workers (Black et al. 1998). and the present work differ roughly by the same amount. Close to threshold, however, the sixteen-state calculations show no sign of the rapid rise (cf Figure 3) demonstrated by Black and co-workers (Black et al. 1998) which appears

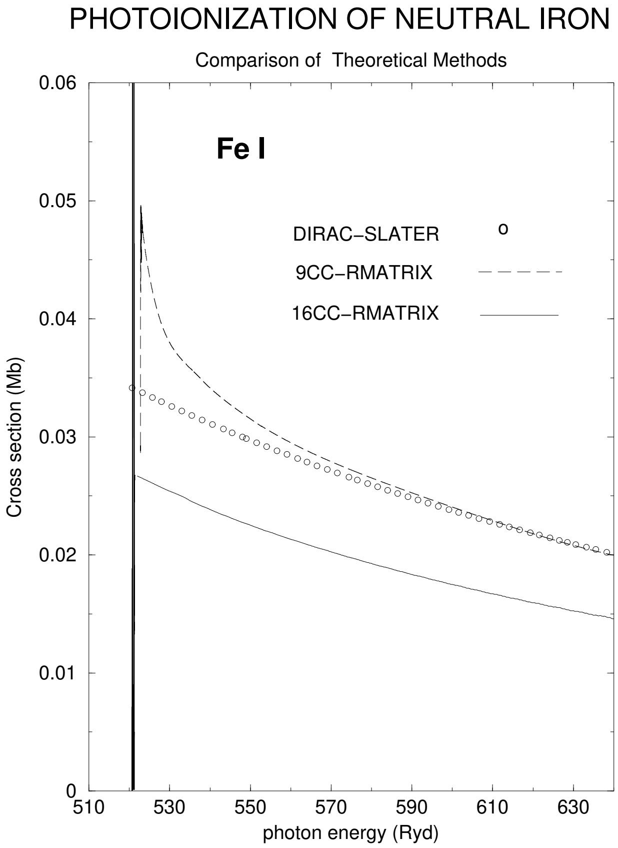

Figure 3. Total cross sections for the 1s photoionization of the ground state of neutral iron. Solid line is the 16-state results, at all energies (Rydbergs), dashed line is that from the 9-state work (Black et al. 1998) and the open circles are those from the relativistic central field approximation (Verner et al. 1993).

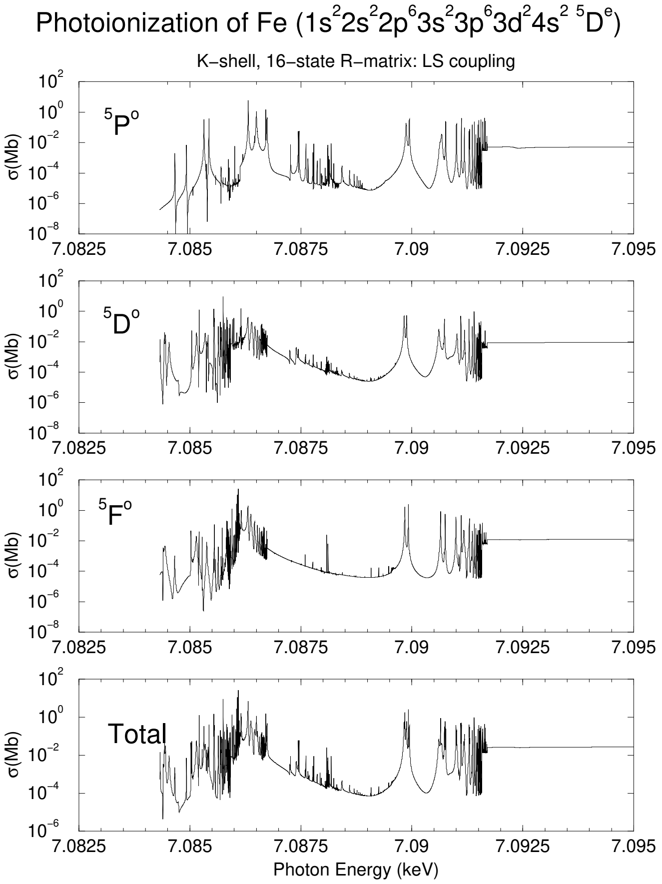

Figure 4. Partial and total cross sections from the sixteen-state R-matrix results performed in LS-coupling. The wealth of resonance structure in the photon region above the K-edge is clearly illustrated.

to have been replaced by the resonance structure as illustrated in Figure 4. The explanation for this significant reduction in the background cross section is related to the degree of configuration interaction included in the various calculations and it should be stressed that the nine-state calculation includes the $1s^{-1}3d^64s^2\ ^6D$ and $1s^{-1}3d^64s^2\ ^6D$ by only a single configuration and neglected any electron correlation effects which are deemed to be important.

We note that the inclusion of configuration interaction gives rise to eigenvector coefficients corresponding to the configurations (i.e. $1s^{-1}3d^64s^2\ ^6D$ and $1s^{-1}3d^64s^2\ ^4D$) which are substantially less than unity. The remaining configurations in the eigenvector expansions do not contribute significantly to the partial cross section. Configuration interaction effects gives rise to the reduction in the total cross section. The agreement between the length and velocity formulations is highly satisfactory but this is not a fool proof method for verifying the accuracy of the cross sections. A rough estimate of the accuracy of the present work can be gauged from the experimental work on the structurally similar neutral nickel system (Parthasaradhi et al. 1998). The spectrum of neutral Ni near its K-edge is similar to that resolved in the present work. Secondly, Wang Dachun and co-workers (Wang et al. 1992) have experimentally determined the X-ray attenuation coefficients for neutral Fe which allow the calculation of the *total* cross section at the threshold. Examination of the neutral Fe experimental data before and after threshold gives us a rough value of the $1s$ cross section which unfortunately also includes electron scattering contributions. While experimental results are within 20% of the present work, it is not possible to draw conclusions from these data about the accuracy of our calculation.

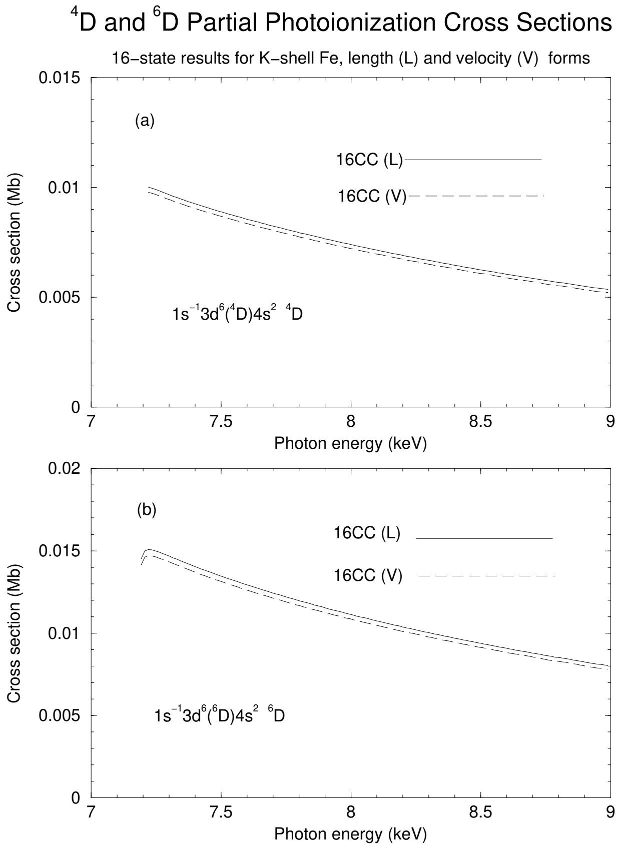

Figure 5. Length and velocity forms of the partial cross sections for the 1s photoionization of the ground state of neutral iron, leaving the resulting Fe^+ ion in the (a) $1s^{-1}3d^6 4s^2\ ^4D$ and (b) $1s^{-1}3d^6 4s^2\ ^6D$ hole states.

5. Future Work

The discussion on the K-shell photoionization of neutral Fe presented above concentrated on including only the $1s^{-1}$ hole states. It is clear from the various investigations presented above that there are many limitations of these calculations. First and foremost is the fact that only the Fe^+ $1s^{-1}$ hole states are included in both the nine and sixteen-state R-matrix calculations, whereas the valence states of Fe^+ are totally neglected. This may be suitable if one is primarily interested in energies above the K-edge. However neglecting the valence states effectively discounts the structure approaching the K-edge from below. Their inclusion is of importance if one is interested in calculating the optical constants f_1 and f_2 from the photoabsorption cross sections for applications (Henke et al. 1993). The majority of ab initio calculations to date have been carried out in LS - coupling. There is very limited work which takes into account relativistic effects, which are clearly important for the neutral iron system. The work of Verner and co-workers (Verner et al. 1993) attempts to cater for relativistic effects admittedly within the confines of the Dirac-Slater approach at the single configuration level but this work totally neglects any resonances effect. A thorough study where both relativistic and correlation effects are included in the theoretical model is required. Such relativistic effects can be investigated within the context of the R-matrix approach, either at the Breit-Pauli level or within a fully Dirac approach and are presently being investigated. If one envisages including valence and hole states of Fe^+ other than $1s^{-1}$ then the limitations of present day computer architectures will be the major factor which curtails the number of states included in any calculation. Furthermore, investigation into the size of the basis set required has

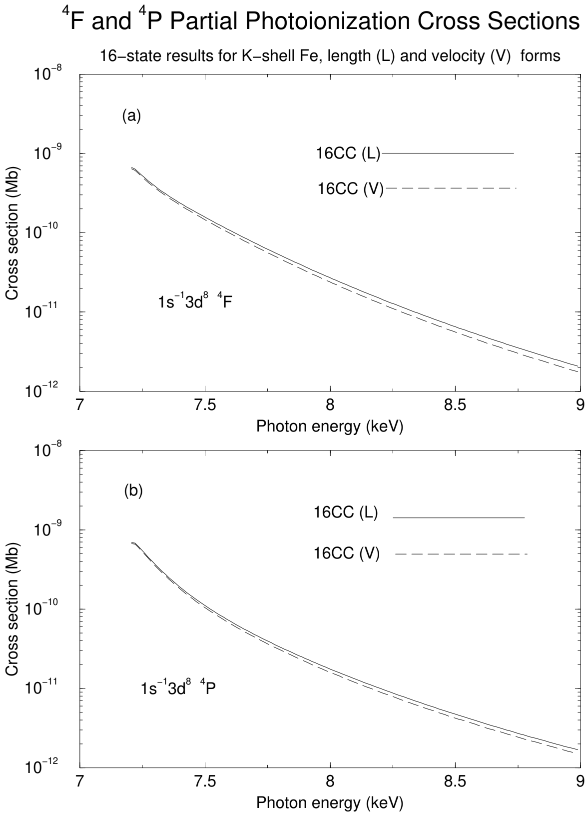

Figure 6. Length and velocity forms of the partial cross sections for the 1s photoionization of the ground state of neutral iron, leaving the resulting Fe^+ ion in the (a) $1s^{-1}3d^8\ {}^4F$ and (b) $1s^{-1}3d^8\ {}^4P$ hole states.

to be addressed so that highly correlated targets state of Fe^+ can be included, when additional hole and valence states are included. Finally the numerical stability of the continuum basis regarding the number of terms required to span the 7 keV range between the ground state and the $1s^{-1}$ hole states of singly ionized iron is another fundamental problem to be addressed.

6. Summary

The status of K-shell photoionization of neutral iron has been reviewed. A comparison with the available (although limited) experimental data and existing theoretical work is made for this important element. Several anomalies and features are illustrated and future directions of theoretical work are indicated. We have presented the results from the current '*state of the art*' ab initio R-matrix calculations for K-shell photoionization of neutral iron. Resonance structure near threshold has been fully resolved and a background approximately 25% lower than previous work has been determined, the difference being attributed to correlation effects in the target. It should be emphasized that the results reported are not definitive and more extensive calculations are still required. A more *definitive* calculation would ideally include a large number of 'hole'-states together with valence states. However, we have shown the importance of including correlation effects on the background total cross section.

Acknowledgments. The work reported on here was supported by grants from the UK PPARC program. BMMCL would like to thank a number of people; Dick Edgar, Douglas Swartz, John Houck, John Raymond and Randall Smith for many intensive discussions which contributed to this article.

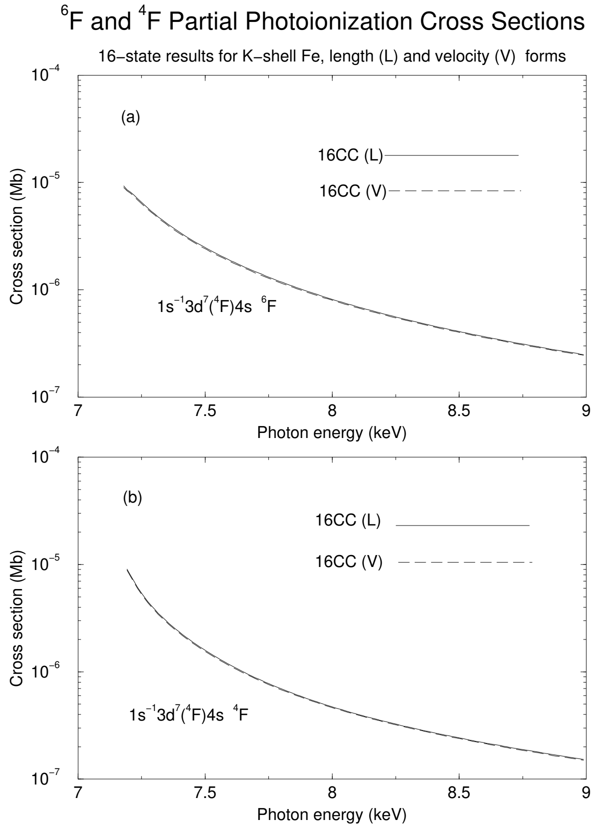

Figure 7. Length and velocity forms of the partial cross sections for the 1s photoionization of the ground state of neutral iron, leaving the resulting Fe^+ ion in the (a) $1s^{-1}3d^7 4s\ ^6F$ and (b) $1s^{-1}3d^7 4s\ ^4F$ lowest hole states.

References

Bai, T. 1979, Sol. Phys. 62, 113, *erratum* Sol. Phys. 64, 417.

Bautista, M.A. and Pradhan, A.K. 1995, J. Phys. B: At. Mol. & Opt. Phys.28, L173.

Black, G.M., Donnelly, D., Bell, K.L., Scott. M.P., and Keenan, F.P. 1998, Astron. and Astrophys. 337, L21.

Burke, P.G. and Berrington, K.A. (eds.) 1993, "Atomic and Molecular Processes an R-matrix Approach" (Bristol : IOP Publishing).

Clementi, E. and Roetti, C. 1974, At. Data Nucl. Data Tables 14, 177.

Donnelly, D., Bell, K.L., Scott, M.P., Keenan, F.P., and McLaughlin, B.M. 1999, X99 contributed papers:(http://www.phy.anl.gov/X99), *X-ray and Inner-shell Processes*, 154.

Donnelly, D., Bell, K.L., Scott, M.P., and Keenan, F.P. 2000, ApJ 531, 1168.

Henke, B.L., Gullikson, E.M., and Davis, J.C. 1993, At. Data. Nucl. Data Tables 54, 181.

Hibbert, A. 1975, Comput. Phys. Commun. 11, 141.

Mushotzky, R.F., Done, C. and Pounds, K.A. 1993, Ann. Rev. Astron. and Astrophys. 31, 717.

Parmar, A.N., Wolfson, C.J., Culhane, J.L., Phillips, K.J.H., Acton, L.W., Dennis, B.R., and Rapley, C.G. 1984, ApJ 279, 866.

Parthasaradhi, K., Esposito, A., Mobilio, S., and Pelliccioni, M. 1998, Phys. Rev. A 38, 1608.

Phillips, K.J.H., Pike, C.D., Lang, J., Watanabe, T., and Takahashi, M. 1994, ApJ 435, 888.

Servier, K.D. 1979, At. Data. Nucl. Data Tables 24, 323.

Verner, D.A. and Yakovlev, D.G. 1995, Astron. and Astrophys. Suppl. 109, 125.

Verner, D.A., Yakovlev, D.G., Band, I.M., and Trzhaskovskaya, M.B. 1993, At. Data Nucl. Data Tables 55, 233.

Wang, D., Ding, X., Wang, X., Yang, H., Zhou, H., Shen, X., and Zhu, G. 1992, Nucl. Instr. Meth. Phys. Res. B 71, 241.